Stability of Cable-Stayed Bridge with Composite I-Girder Under Dynamic Wind Loads Using Computational Fluid Dynamics (CFD)

Danny Sahusilawane, Bambang Supriyadi, Akhmad Aminullah

Department of Civil and Environmental Engineering, Universitas Gadjah Mada, Yogyakarta, INDONESIA

E-mail: dannysahusilawane@mail.ugm.ac.id, Bambang.supri@ugm.ac.id, akhmadaminullah@ugm.ac.id

| Submitted: September 20, 2025 | Revised: October 09, 2025 | Accepted: August 04, 2026 |

| Published: September 15, 2026 |

ABSTRACT

Cable-stayed bridges have emerged as a preferred solution for long-span crossings due to their efficient use of materials and visually appealing design. Nevertheless, their slender aerodynamic configuration renders them highly susceptible to dynamic wind effects such as flutter and vortex shedding, which may compromise serviceability and safety. This study formulates the problem by examining the aerodynamic stability of a composite I-girder cable-stayed bridge under varying wind speeds through the application of Computational Fluid Dynamics (CFD). The bridge deck, with a main span of 150 m, was modeled in three-dimensional solid form and subjected to wind speeds of 4, 8, 12, and 25 m/s. Modal analysis indicated that the torsional-to-bending frequency ratio (ft/fb) was 1.61, falling below the minimum requirement of 2.5 set by Indonesian Bridge and Road Guidelines No. 02/P/BM/2022, thereby justifying further aerodynamic assessment. The novelty of this research lies in integrating structural modal analysis with CFD-based simulations under site-specific wind conditions, providing insights rarely explored in regional contexts. Results demonstrated that the stability parameter fell within category A for 4 and 8 m/s, where wind effects were negligible, but shifted to category B at 12, 17.8, and 25 m/s, requiring attention to deck cross-section geometry. Vortex shedding patterns at 17.8 m/s were regular and consistent, indicating potential resonance, while flows became increasingly complex at 25 m/s, generating higher aerodynamic forces and turbulence energy. Maximum lateral displacements reached 425.6 mm and vertical displacements up to 388.6 mm at extreme wind speeds. In conclusion, CFD-based numerical analysis proved essential in identifying critical wind-induced responses, confirming its importance as a design-stage tool to ensure the long-term stability and reliability of cable-stayed bridges.

Keywords: cable-stayed bridge, composite I-girder, CFD, stability parameter, wind load.

INTRODUCTION

Cable-stayed bridges represent a vital component of modern transportation infrastructure, offering efficient solutions for long-span crossings while maintaining an aesthetically appealing form. Their slender and flexible configuration has made them increasingly popular in large-scale infrastructure projects. However, these same characteristics also render cable-stayed bridges vulnerable to dynamic wind loads, which may induce vibrations, excessive deformations, or even structural failure under extreme conditions.

Aerodynamic studies during both the design and post-construction phases are therefore indispensable. Dynamic wind actions can trigger oscillations that threaten the safety and serviceability of the structure. The historical collapse of the Tacoma Narrows Bridge in 1940 remains a pivotal lesson in the importance of integrating aerodynamics into bridge engineering. Among the analytical tools available, Computational Fluid Dynamics (CFD) has emerged as an effective numerical method for evaluating wind–structure interactions, including vortex formation, flow patterns around bridge decks, and structural responses to aerodynamic forces.

CFD provides detailed insights into pressure distribution, velocity fields, and turbulence energy that are difficult to obtain solely through experimental testing. Moreover, it allows for efficient and cost-

pISSN 2302-4240
eISSN 2655-2086
Volume 15, Issue 3, September 2026, pp.0768-0780
DOI: http://dx.doi.org/10.32832/astonjadro.v15i3.21590 http://ejournal.uika-bogor.ac.id/index.php/ASTONJADRO

effective analysis of cable arrangements, deck geometries, wind angles of attack, and various wind scenarios. For the sustainable and safe design of bridges in the digital era, integrating structural modeling with fluid simulations has become essential. In this research, the objective is to evaluate the dynamic response of a composite I-girder cable-stayed bridge under varying wind speeds.

The novelty of this study lies in combining structural modal analysis with CFD simulations under site-specific wind conditions in Ambon Bay, Indonesia—an aspect rarely addressed in regional bridge studies. By identifying that the torsional-to-bending frequency ratio falls below the required threshold of Indonesian standards, this research underscores the need for advanced aerodynamic assessment. The results are expected to provide valuable insights for enhancing both local practice and broader design guidelines.

RESEARCH METHODS

Bridge Data

The geometric characteristics of the bridge were determined based on detailed structural data. The bridge has an overall span length of 300 meters, consisting of a main span measuring 150 meters and two side spans of 75 meters each. The reinforced concrete deck slab was designed with a thickness of 0.25 meters, supporting the composite girder system. The bridge provides a total width of 21.5 meters, ensuring adequate capacity for traffic lanes and auxiliary functions. The pylon towers rise to a height of 83.5 meters, serving as the primary vertical support for the cable-stayed system. Meanwhile, the girder depth is 2.30 meters, contributing to the stiffness and overall load-bearing capacity of the deck. These dimensional properties form the fundamental basis for structural modeling and aerodynamic analysis in this study. Table 1 presents the material properties of the cable-stayed bridge structure. The geometry of the girder and cross beam is illustrated in Figure 1.

Table 1. Types and grades of materials used in the cable-stayed bridge

Component	Material	Grade / Strength
Pylon	Reinforced Concrete	f'c = 40 MPa
Bridge Deck	Steel IWF Section	fy = 345 MPa; fu = 450 MPa
Cable	Prestressing Steel Strands	ASTM A416-06, Grade 270

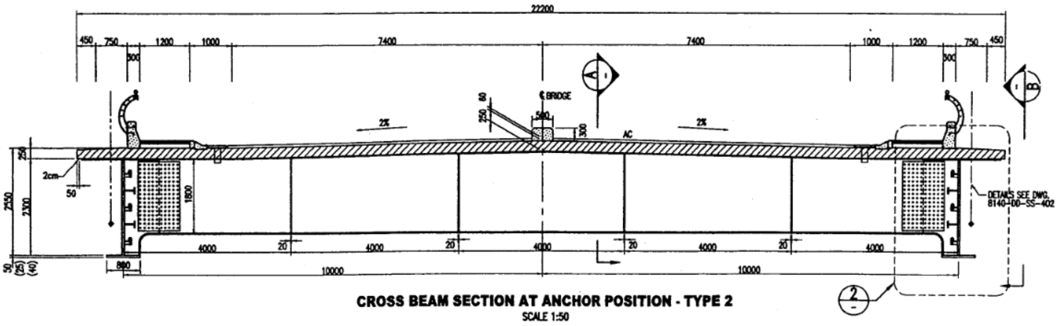

Figure 1. Geometry of the main girder and cross beam of the cable-stayed bridge structure

Wind Speed Data

The daily wind data for Ambon City covering the two-year period of 2023–2024 were obtained from the official meteorological database of the Indonesian Agency for Meteorology, Climatology, and Geophysics (BMKG). The analysis was conducted using the WRPlot software, with the results illustrated in Figure 2. The frequency distribution reveals that wind speeds in the range of 0.50–2.10 m/s occurred at 1.40%, while wind speeds of 2.10–3.60 m/s occurred at 19%. The most dominant wind speed categories were 3.60–5.70 m/s, with a frequency of 34.9%, and 5.70–8.80 m/s, with a frequency of 38.4%. Meanwhile, wind speeds of 8.80–11.10 m/s occurred at 5.90%, and wind speeds exceeding 11.10 m/s occurred at only 0.40% of the total observations.

Based on this frequency distribution, representative wind speeds of 4 m/s, 8 m/s, and 12 m/s were selected for the numerical simulations in this study, along with an extreme wind condition of 25 m/s to evaluate the bridge's aerodynamic stability under critical loading scenarios.

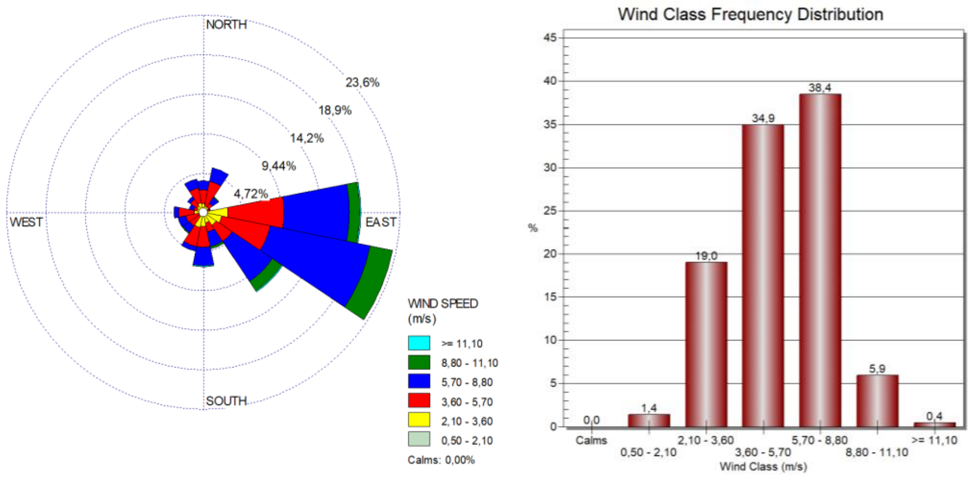

a. Wind Rose b. frequency distribution of wind speeds

Figure 2. Wind rose (a) and frequency distribution of wind speeds (b) in Ambon City during 2023–2024 based on WRPlot analysis

Computational Fluid Dynamics (CFD) Simulation

The software employed for the CFD simulations in this study was Cradle CFD 2024.1 Student Edition. The length considered in the model corresponded to the main span of 150 meters, which was taken as the representative scale for the analysis. The girder was assumed to remain fixed, serving as an idealized representation of the bridge deck subjected to wind flow.

The boundary conditions were defined following the guidelines of British Standard (2005) and PD 6688-1-4:2015 BSI [1], where the velocity inlet was specified at the upstream boundary, the pressure outlet was applied at the downstream boundary, slip wall conditions were assigned to the remaining outer walls, and a no-slip wall condition was imposed on the surface of the bridge deck girder. The geometric parameters of B and D, representing the width and depth of the girder, are illustrated in Figure 3.

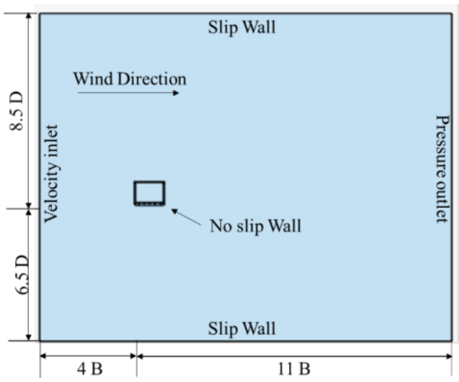

Figure 3. Boundary conditions were defined following the guidelines of British Standard (2005) and PD 6688-1-4:2015 BSI

For the inflow conditions, daily wind speed data from BMKG were adopted together with the critical vortex shedding velocity to ensure realistic aerodynamic loading scenarios. The flow was modeled

Volume 15, Issue 3, September 2026, pp.0768-0780
DOI: http://dx.doi.org/10.32832/astonjadro.v15i3.21590 http://ejournal.uika-bogor.ac.id/index.php/ASTONJADRO

as incompressible, and the k-ω SST turbulence model was employed to capture near-wall effects and accurately represent the complex turbulent flow behavior around the bridge deck.

Bridge Structural Modeling Using Midas Civil

The cable-stayed bridge was structurally modeled using Midas Civil 2024 Student Version to evaluate its dynamic behavior under wind loading. The modeling process was followed by the determination of boundary conditions to accurately represent the structural constraints of the system.

As illustrated in Figure 4, the girder support at the pylon was assigned a translational restraint in the y-direction, which serves as resistance against lateral wind forces. On the left side of the bridge, translational movement was restrained solely in the z-direction, while rotational restraints were applied in all three axes (x, y, and z). Furthermore, the pile cap support was defined as a fixed support condition, providing complete restraint against both translational and rotational degrees of freedom.

This configuration reflects realistic structural behavior by ensuring that the bridge model is properly constrained while maintaining sufficient flexibility to simulate wind-induced responses.

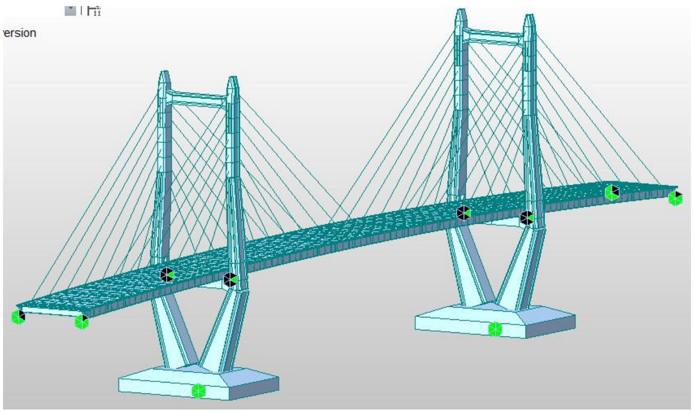

Figure 4. Structural modeling and boundary conditions of the cable-stayed bridge

Natural Frequencies and Stability Parameters

Through the structural modeling of the cable-stayed bridge using MIDAS Civil 2024, a modal analysis was carried out to identify the natural frequencies of the structure and to assess its dynamic response. The results showed that the first vertical bending frequency (fb) was obtained at Mode Shape 1 with a value of 0.672 Hz, while the first torsional frequency (ft) appeared at Mode Shape 6 with a value of 1.084 Hz. The ratio between torsional and bending frequencies (ft/fb = 1.61) was notably lower than the minimum threshold of 2.5 as specified in the Guidelines for Roads and Bridges No. 02/P/BM/2022 (Ministry of Public Works and Housing, 2022). This shortfall indicates that the bridge does not comply with the required standard and therefore warrants more detailed aerodynamic investigations.

A similar issue has been documented in both field measurements and analytical modeling of the Merah Putih Bridge in Ambon, where the first vertical bending frequency (0.660 Hz) was reported to be very close to the first torsional frequency (0.800 Hz) [2], [3]. Such proximity between modes reinforces the risk of resonance phenomena in long-span cable-stayed bridges. Taken together, these findings stress the necessity of performing aerodynamic stability analyses that address critical aeroelastic effects—including vortex shedding, galloping, and flutter—in order to ensure the safety, serviceability, and long-term adequacy of bridge designs.

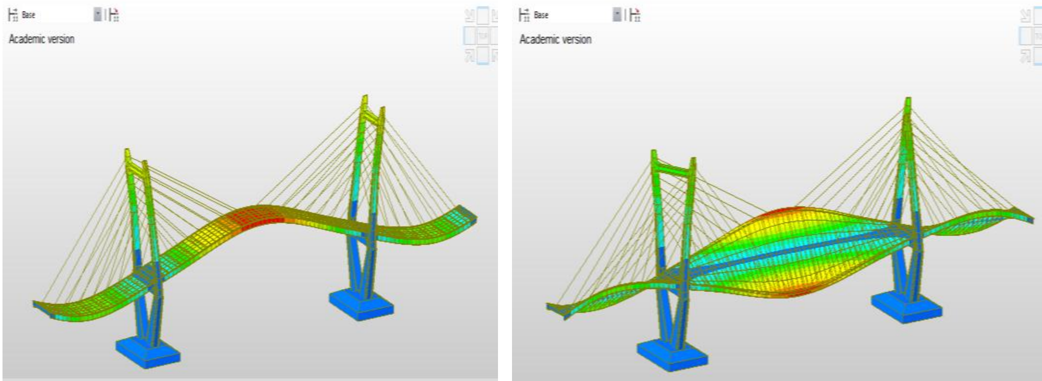

a. bending behavior b. torsional behavior

Figure 5. Mode shapes of the cable-stayed bridge: (a) bending behavior and (b) torsional behavior

The phenomenon of vortex shedding in fluid mechanics arises when airflow interacts with bridge components such as decks or cables, producing alternating periodic vortices on either side of the structure. When inadequately controlled, this process can significantly modify the aerodynamic forces acting on the bridge, potentially inducing unwanted vibrations and, in extreme situations, causing structural instability or failure. The behavior of vortices in bridge girders has been systematically investigated by Von Karman (Walther, 1999) [4], who introduced the use of the Reynolds number (Re) and the Strouhal number (S) as key dimensionless parameters to describe and predict vortex characteristics. The mathematical representation of these parameters can be expressed as follows:

$$\mathrm{v} = \left(\frac{\mathrm{fb\ x\ h}}{\mathrm{S}}\right) \qquad\qquad R_e = \frac{V\ x\ B}{\nu}$$

where fb is the natural bending frequency, h is the height of the vehicle deck, S is the Strouhal number with values typically ranging between 0.10 and 0.20, v is the wind speed (m/s), B is the bridge deck width (m), ν is the kinematic viscosity of air (≈ 0.15 cm^2/s), and Re is the Reynolds number (in the order of 10^5–10^7).

Wind vortices or turbulence occur at certain wind speeds, inducing resonance and amplifying the vibration response of the structure. From the calculation of Equation (1) using a Strouhal number of 0.10, the critical wind speed at which vortex shedding occurs was determined to be 17.80 m/s. Subsequently, the vortex effect was evaluated using the Reynolds number (Re). The Reynolds number must satisfy specific requirements because it depends on the acting wind speed, with the acceptable range being 10^5–10^7. Based on the calculation of Equation (2), the Reynolds number was obtained as 2.55×10^7, which exceeds the upper limit of 10^7, indicating that the airflow is highly turbulent. This turbulence arises because inertial forces dominate, causing the fluid to move in a highly irregular manner, significantly overpowering the viscous forces that would otherwise act to stabilize the flow.

(Ministry of Public Works and Housing, 2015) in the Technical Guidelines for Cable-Stayed Bridges [5] explains that the level of bridge vulnerability to dynamic wind loads is expressed by the parameter Pb, as follows:

$$\mathrm{Pb} = \left(\frac{\phi \mathrm{b}^2}{\mathrm{m}}\right)\left(\frac{16\mathrm{V}^2}{\mathrm{bLfb}^2}\right)$$

where ϕ is the air density = 1.3 (kg/m^3), b is the total width of the bridge deck (m), m is the bridge weight per unit length (kN/m), V is the average wind speed over a one-hour period (m/s), L is the maximum span length (m), and fb is the natural bending frequency (Hz). The classification of bridge vulnerability levels to dynamic wind loads is presented in Table 2.

pISSN 2302-4240
eISSN 2655-2086
Volume 15, Issue 3, September 2026, pp.0768-0780
DOI: http://dx.doi.org/10.32832/astonjadro.v15i3.21590 http://ejournal.uika-bogor.ac.id/index.php/ASTONJADRO

Table 2. Types and grades of materials used in the cable-stayed bridge

Category Type	Condition	Description
Category A	Pb < 0.04	The influence of dynamic wind on the bridge structure is not significant.
Category B	0.04 ≤ Pb ≤ 1	Attention is required regarding the cross-sectional shape of the bridge.
Category C	Pb > 1	The influence of dynamic wind is highly significant.

Based on the wind conditions observed at the bridge site, the wind speed data were found to range between 4, 8, and 12 m/s, with an extreme wind speed of 25 m/s. Corresponding to these wind speed values, the dynamic wind stability parameters of the bridge are presented in Table 3 and Figure 6.

Table 3. Dynamic wind stability parameters of the bridge

Wind Speed (m/s)	Stability Parameter (Pb)	Category
4	0.0050	Category A
8	0.0199	Category A
12	0.0448	Category B
17.80	0.0986	Category B
25	0.1945	Category B

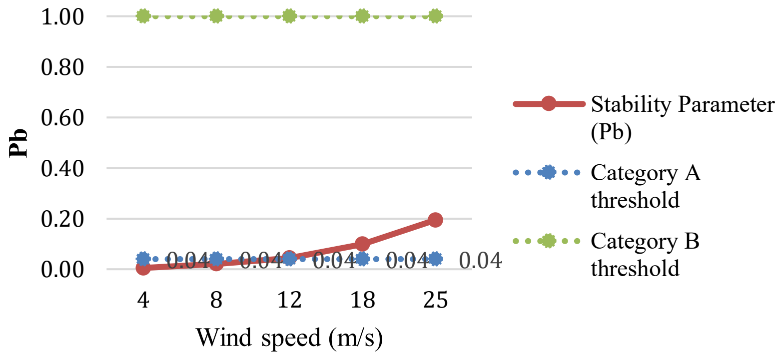

Figure 6. Dynamic wind stability parameters of the bridge

The assessment of the dynamic wind stability parameter offers a deeper understanding of how the cable-stayed bridge performs aerodynamically under different wind regimes. As illustrated in Table 3 and Figure 6, the parameter remains within Category A when wind speeds are 4 m/s and 8 m/s, signifying that the influence of dynamic wind forces on the bridge structure is minimal. Under these conditions, the bridge can be considered to operate safely in low to moderate wind environments without raising significant aerodynamic concerns.

When wind speeds increase to 12 m/s, 17.80 m/s, and 25 m/s, however, the stability parameter shifts to Category B. This transition indicates that the geometry of the bridge deck cross-section becomes a decisive factor affecting overall stability. The movement into Category B reflects the growing presence of critical aerodynamic phenomena, including vortex shedding and elevated turbulence intensity, both of which can magnify the structural response and heighten the potential for dynamic instabilities.

These results underscore that although the bridge remains sufficiently stable at lower wind velocities, greater attention must be devoted to the design and refinement of the deck profile when high wind conditions are considered. Careful adjustments to geometric detailing and structural configuration are therefore vital to ensure the bridge's resilience. Ultimately, the findings confirm that the aerodynamic stability of cable-stayed bridges is strongly dependent on wind speed, and long-term safety under severe wind scenarios requires rigorous optimization of both structural form and aerodynamic design.

Results of CFD Simulation

The computational simulations carried out using Cradle CFD 2024.1 employed multiple wind speeds under both steady-state and transient flow conditions. The wind speeds analyzed were 4 m/s, 8 m/s, 12 m/s, and 25 m/s, representing typical to extreme scenarios observed at the bridge site. These simulations enabled detailed visualization of the airflow patterns around the bridge deck, with particular emphasis on the phenomenon of vortex shedding.

At t = 100 seconds, the simulation results revealed a marked contrast in vortex behavior between wind speeds of 17.80 m/s and 25 m/s. For the case of 17.80 m/s, the vortex shedding patterns appeared regular and consistent, highlighting a critical condition in which resonance may occur when the vortex shedding frequency coincides with the natural frequency of the structure. Conversely, at 25 m/s, the airflow developed into a more complex pattern, with velocity magnitudes near the upper and lower surfaces of the deck increasing from 25 m/s to 28 m/s. This escalation indicates the presence of extreme wind loading conditions, generating significantly greater aerodynamic forces acting on the bridge deck.

In addition, the analysis demonstrated that turbulence energy intensifies as wind speed increases. The maximum turbulence energy was found to be 0.228 m^2/s^2 at 17.80 m/s, and slightly higher at 0.229 m^2/s^2 for 25 m/s. Although the numerical difference appears minor, the nonlinear nature of aerodynamic effects at such wind speeds amplifies structural responses. These findings, presented in Figures 7 and 8, underscore the importance of accounting for nonlinear aerodynamic behavior at high wind velocities in the design and stability assessment of cable-stayed bridges.

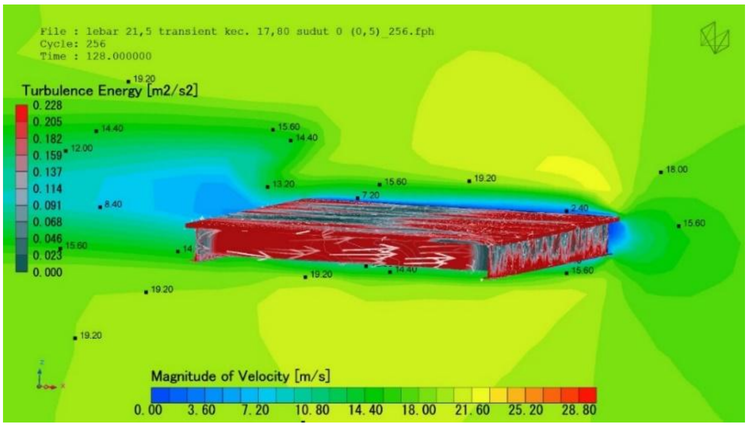

Figure 7. Vortex shedding pattern obtained from the 17.80 m/s simulation at t = 100 seconds

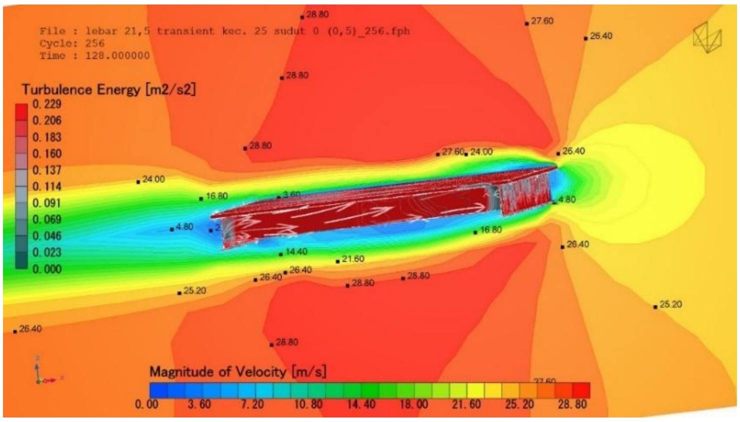

Figure 8. Vortex shedding pattern obtained from the 25 m/s simulation at t = 100 seconds

In addition, the simulation results also encompassed the analysis of forces and moments, which were evaluated to understand the structural response of the cable-stayed bridge. The findings indicate that

pISSN 2302-4240
eISSN 2655-2086
Volume 15, Issue 3, September 2026, pp.0768-0780
DOI: http://dx.doi.org/10.32832/astonjadro.v15i3.21590 http://ejournal.uika-bogor.ac.id/index.php/ASTONJADRO

the largest forces occur in the transverse direction (Y-axis), while the largest moments are concentrated in the vertical direction (Z-axis). At a wind speed of 4 m/s and 8 m/s, the maximum transverse force in the Y-direction occurred at t = 0.5 seconds, reaching 31.3 kN and 62.6 kN, respectively. At subsequent time steps, these values decreased to 4.5 kN and 17.5 kN. For a wind speed of 12 m/s, the maximum Y-direction force was recorded at t = 1.5 seconds, with a magnitude of 100.73 kN, which then reduced to 39.5 kN in later stages. At the extreme condition of 25 m/s, the maximum Y-direction force occurred at t = 2.5 seconds, reaching 290.3 kN, while subsequent values decreased to 170.5 kN.

Similarly, the results for the vertical moment (Z-axis) revealed increasing magnitudes with higher wind speeds. At 4 m/s and 8 m/s, the maximum Z-direction moments were observed at t = 0.5 seconds, amounting to 2350 kN·m and 4700.56 kN·m, respectively. At later time intervals, these values decreased to 340 kN·m and 1315 kN·m. For a wind speed of 12 m/s, the maximum vertical moment reached 7561.88 kN·m at t = 1.5 seconds, subsequently reducing to 2975 kN·m. At 25 m/s, the maximum vertical moment was recorded at 21,773 kN·m at t = 2.5 seconds, later decreasing to 12,975 kN·m.

These results clearly demonstrate that wind speed has a substantial influence on the magnitude of both forces and moments, which in turn may induce significant structural vibrations and lift forces on the bridge deck. Such effects are illustrated in Figures 9 and 10, emphasizing the importance of considering wind-induced responses in the aerodynamic design and safety evaluation of cable-stayed bridges.

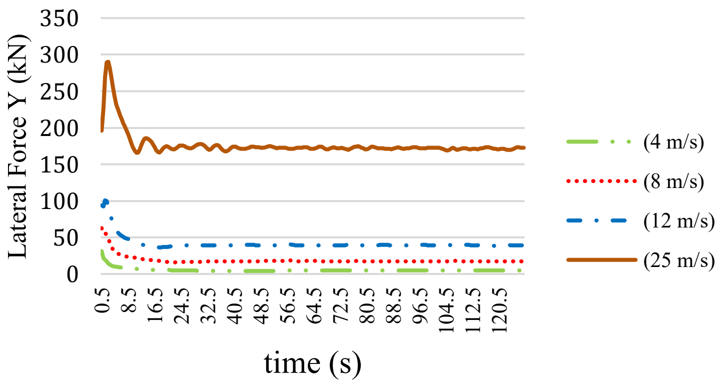

Figure 9. Force in the Y-direction on the bridge deck at wind speeds of 4, 8, 12, 25 m/s

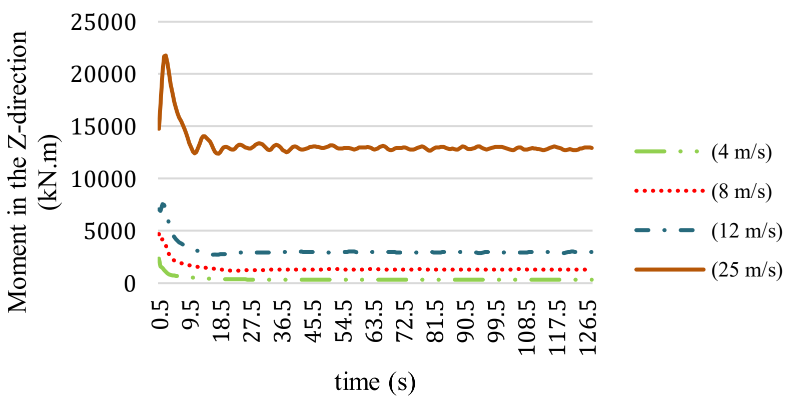

Figure 10. Moment in the Z-direction on the bridge deck at wind speeds of 4, 8, 12, and 25 m/s

Bridge Structural Response

Subsequently, the calculated forces and moments were applied to the structural bridge model developed in Midas Civil 2024 using a time history analysis approach. The variation of forces and moments with respect to time was incorporated as dynamic loading through the nodal dynamic feature of the software. At a wind speed of 25 m/s, the resulting displacements were found to be highly significant, particularly in the transverse direction (Y-axis) and the gravitational direction (Z-axis).

For the Y-axis response, the maximum displacement occurred at t = 1 second with values of 44.80 mm and 97.81 mm for wind speeds of 4 m/s and 8 m/s, respectively. At higher wind speeds of 12 m/s and 25 m/s, the maximum displacement occurred at t = 2.5 seconds, reaching 155.30 mm and 425.60 mm, respectively. In subsequent time steps, the average Y-direction displacements were recorded as 5.58 mm, 20.55 mm, 45.34 mm, and 194.91 mm for wind speeds of 4 m/s, 8 m/s, 12 m/s, and 25 m/s, respectively.

For the Z-axis response, the maximum displacement at t = 1.5 seconds was 17.17 mm for the 4 m/s case, while at t = 3 seconds, the displacements were 59.89 mm, 120 mm, and 388.60 mm for wind speeds of 8 m/s, 12 m/s, and 25 m/s, respectively. In the subsequent time steps, the average Z-direction displacements were found to be –0.90 mm, 3.23 mm, 10.51 mm, and 62.16 mm for wind speeds of 4 m/s, 8 m/s, 12 m/s, and 25 m/s, respectively.

The displacement responses at the midspan of the main bridge (node 1274) are further illustrated in Figures 11 and 12, which provide a clearer depiction of the bridge's structural behavior under dynamic wind loading.

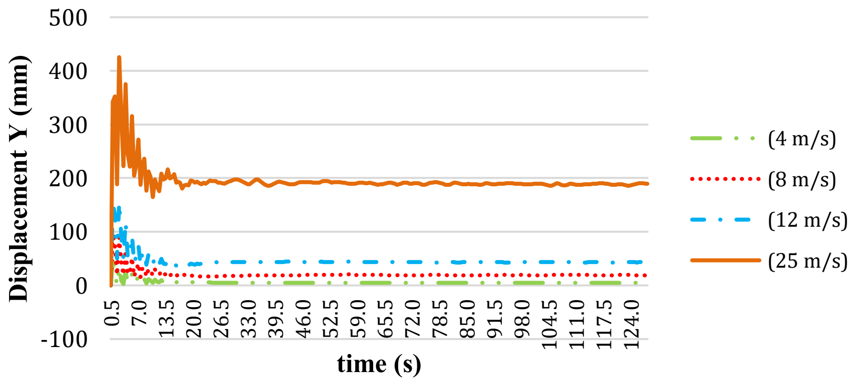

Figure 11. Y-direction displacement at the mid-span of the main span under different wind speeds

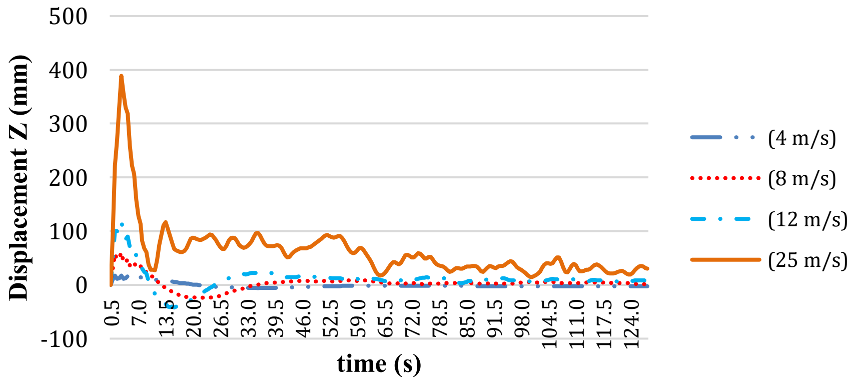

Figure 12. Z-direction displacement at the mid-span of the main span under different wind speeds

pISSN 2302-4240
eISSN 2655-2086
Volume 15, Issue 3, September 2026, pp.0768-0780
DOI: http://dx.doi.org/10.32832/astonjadro.v15i3.21590 http://ejournal.uika-bogor.ac.id/index.php/ASTONJADRO

RESULT AND DISCUSSION

The modal analysis conducted in this study revealed that the torsional-to-bending frequency ratio (ft/fb) was only 1.61, which is significantly lower than the minimum threshold of 2.5 required [6]. This shortfall highlights the susceptibility of the bridge to resonance phenomena, given the close proximity between the first vertical bending frequency (0.672 Hz) and the first torsional frequency (1.084 Hz). Similar observations were reported in the Merah Putih Bridge in Ambon, where modal frequencies of 0.660 Hz and 0.800 Hz were found to be closely spaced, increasing the likelihood of resonance [2], [3]. These findings are consistent with the work [7], who emphasized that low ft/fb ratios heighten aeroelastic instability in Π-type composite girders, and with Badhurshah et al. (2024), who showed that insufficient separation between modal frequencies in twin-box girders intensifies aeroelastic coupling, thereby reducing safety margins in long-span designs [8]. Recent studies on the Xiangshan Harbor Cable-Stayed Bridge also confirmed that inadequate frequency separation significantly lowers flutter reliability, underscoring the importance of modal control in bridge design [9].

The onset of vortex shedding was identified at a critical velocity of 17.8 m/s, where periodic and stable vortex patterns were observed. Such conditions are particularly concerning because they align closely with the natural frequencies of the structure, creating the potential for resonance. This phenomenon supports the findings, who noted that inhomogeneous wind fields tend to accelerate the onset of aeroelastic oscillations in cable-stayed bridges [10]. As wind velocity increased further to 25 m/s, the flow patterns became considerably more complex, with local wind accelerations recorded at up to 28 m/s above the deck surface, reflecting extreme turbulence. These results are consistent, who demonstrated that turbulence intensification significantly magnifies lift forces and torsional moments, thereby exacerbating aerodynamic instabilities [11]. In addition, found that clearance and proximity effects could trigger premature vortex shedding even at moderate wind speeds, further illustrating the sensitivity of bridge decks to boundary conditions [12].

The aerodynamic stability assessment based on the stability parameter (Pb) further reinforces these concerns. While the bridge remained in Category A at wind speeds of 4 m/s and 8 m/s—conditions under which wind-induced effects are negligible-it transitioned to Category B at 12 m/s, 17.8 m/s, and 25 m/s. This shift indicates that at higher wind velocities, the geometric characteristics of the deck become decisive in determining stability. This observation corresponds, who demonstrated that the aerodynamic stability of suspension and cable-supported bridges during construction is heavily dependent on cross-sectional geometry, which can be optimized to improve performance [13]. Also noted that small static angles of attack, such as a slight “nose-up” orientation, can elevate critical flutter speeds, underscoring the importance of fine-tuning deck aerodynamics during the design stage [14].

The CFD simulations revealed further evidence of nonlinear aerodynamic escalation. At 25 m/s, the maximum transverse force acting on the deck reached 290.3 kN, while the torsional moment peaked at 21,773 kNm. These values represent a sharp increase compared with the 12 m/s condition, underscoring the nonlinear relationship between wind velocity and aerodynamic response. Such patterns align with the findings of Fan et al. (2022), who identified that aerodynamic interference among parallel girder configurations generates nonlinear distributions of aerodynamic forces [15]. Showed that once wind speeds surpass critical thresholds, displacement responses grow nonlinearly, potentially leading to lock-in phenomena characterized by prolonged vibration cycles [16]. Long-term evaluations of flutter reliability also indicate that such risks can accumulate across the life cycle of the bridge, as degradation and environmental changes alter modal properties and reduce safety margins [17].

The structural responses corroborated these aerodynamic findings. At the extreme wind speed of 25 m/s, transverse displacement at midspan reached 425.6 mm, while vertical displacement was measured at 388.6 mm—an order of magnitude greater than the 44.8 mm displacement recorded at 4 m/s. The quasi-quadratic growth of displacement with wind speed aligns with the work, who demonstrated that flutter and vortex-induced vibrations (VIV) become significantly more pronounced in non-optimized composite girder decks as wind velocity increases [18]. Furthermore, studies by revealed that even environmental factors such as temperature variations can shift modal frequencies in composite cable-stayed bridges, suggesting that the large displacements recorded in this study could become even more critical under combined wind–thermal effects [19]. These results indicate that under critical conditions, the bridge deck would experience excessive dynamic deformations, threatening both structural safety and serviceability.

Beyond the numerical findings, the relevance of this study can be better understood when contextualized with the contributions of Akhmad Aminullah and colleagues, who have advanced methodologies for monitoring and validating dynamic responses in cable-supported bridges. Demonstrated through Enhanced Frequency Domain Decomposition (EFDD) that accurate modal identification is essential for anticipating resonance risks, as shown in their structural health assessment of the Kretek II Bridge [20]. Illustrated that tiltmeters can reliably estimate bridge displacements when processed with interpolation and integration methods, a finding particularly pertinent to the present study where large wind-induced displacements were predicted [21]. Conducted shake table tests on a floating cable-stayed bridge model, revealing that transverse and torsional responses dominate under dynamic excitation, which strongly resonates with the present observation of force and displacement amplification in the transverse direction [22]. These insights also align with recent perspectives on aero-structural design optimization, where nonlinear aeroelasticity-driven approaches are increasingly being adopted to fine-tune deck profiles and enhance flutter stability in long-span bridges [23].

Taken together, this body of evidence paints a coherent picture: cable-stayed bridges with low torsional-to-bending frequency ratios are highly vulnerable to aeroelastic instabilities; vortex shedding is strongly governed by deck geometry and turbulence characteristics; and increasing wind velocities induce nonlinear aerodynamic and structural responses that significantly magnify displacement demands. Importantly, the collective contributions of Aminullah and colleagues bridge the gap between numerical simulations and experimental or field-based validation, underscoring the critical role of structural health monitoring systems-such as tiltmeters and accelerometers-in providing early warnings of lock-in phenomena. Consequently, the present study reinforces the growing consensus in the literature that CFD analyses should be systematically incorporated into the early stages of cable-stayed bridge design, prior to wind tunnel testing, to ensure aerodynamic resilience, serviceability, and long-term reliability of long-span bridge infrastructure.

CONCLUSION

This study confirms that the aerodynamic stability of cable-stayed bridges with composite I-girders is highly sensitive to modal properties and dynamic wind actions, as indicated by a torsional-to-bending frequency ratio of 1.61, below the required threshold of 2.5, and by the onset of vortex shedding at 17.8 m/s with turbulence intensifying at 25 m/s. CFD simulations revealed nonlinear growth of aerodynamic forces, moments, and displacements, with maximum transverse and vertical responses reaching 425.6 mm and 388.6 mm, respectively, underscoring the need for cross-sectional optimization and stability parameter evaluation. By integrating site-specific wind data, modal analysis, and CFD, this research provides new insights into aeroelastic behavior rarely explored in Indonesia, while aligning with international findings and emphasizing the importance of monitoring systems and experimental validation to anticipate resonance and lock-in phenomena. The results highlight that CFD-based evaluations should be systematically adopted in design reviews, particularly for coastal and wind-prone regions, and future research should expand toward multi-hazard assessments to ensure the resilience, safety, and sustainability of long-span bridges.

ACKNOWLEDGEMENT

The author would like to express sincere gratitude to Universitas Gadjah Mada and to the companies that have developed academic versions of software such as Midas Civil and Cradle CFD, which the author was permitted to use in this research. The author also extends appreciation to all parties who have contributed to the successful implementation of this study.

REFERENCES

[1] BRITISH STANDARD, "Eurocode 1 : Actions on structures," 2005, p. Part 1-4: General actions-Wind actions, Committee for 357 Standarization, 3.

[2] Johan Lautan Wijaya Nusantara., Akhmad Aminullah., and Suprapto Siswosukarto., "PENEMPATAN SENSOR AKSELEROMETER PADA JEMBATAN MERAH PUTIH," *J. Tek. Sipil*, vol. 18(1), pp. 21–30, Oktober 2024, doi: 10.24002/jts.v18i1.10354.

[3] Suangga, M., Candra, H., Hidayat, I., and Yuliastuti., "Temperature effect on tension force of stay cable of cable-stayed bridge," *Int. J. Eng. Adv. Technol.*, vol. 9(1), pp. 2251–2257, 2019, doi: 10.35940/ijeat.A9724.109119.

[4] Walther, R., *Cable Stayed Bridges*. London :Thomas Telford, 1999.

[5] Kementerian Pekerjaan Umum dan Perumahan Rakyat, *Pedoman Perencanaan Teknis Jembatan Beruji Kabel, sesuai Surat Edaran No. 08/SE/M/2015*. Jakarta, 2015. [Online]. Available: https://binamarga.pu.go.id/index.php/nspk/detail/pedoman-perencanaan-teknis-jembatan-beruji-kabel

[6] Kementerian Pekerjaan Umum dan Perumahan Rakyat, *02/P/BM/2022 Pedoman Pembahasan Penyelenggaraan Keamanan Jembatan Khusus*. 2022. [Online]. Available: https://binamarga.pu.go.id/index.php/nspk/detail/02pbm2022-pedoman-pembahasan-penyelenggaraan-keamanan-jembatan-khusus

[7] X. Xue, S. Lu, T. Cao, and G. Gao, "A full-cycle aerostatic instability model and the mechanism of Π Composite girder cable-stayed bridges," *Zhendong Yu ChongjiJournal Vib. Shock*, vol. 42, no. 20, pp. 204–213, 2023, doi: 10.13465/j.cnki.jvs.2023.20.024.

[8] R. Badhurshah, A. J. Álvarez, F. Nieto, J. Á. Jurado, and S. Hernández, "Assessment of the Aerodynamic and Aeroelastic Performance of Long-Span Twin-Box Bridges Based upon Multidimensional Surrogate Models," *Appl. Sci.*, vol. 14, no. 13, p. 5531, 2024, doi: 10.3390/app14135531.

[9] H. Zhang, H. Wang, Z. Xu, Y. Zhang, T. Tao, and J. Mao, "Monitoring-based analysis of wind-induced vibrations of ultra-long stay cables during an exceptional wind event," *J. Wind Eng. Ind. Aerodyn.*, vol. 221, 2022, doi: 10.1016/j.jweia.2021.104883.

[10] P. Hu, Y. Han, W. Cheng, G. Xu, and C. S. Cai, "Effects of Inhomogeneous Wind Fields on the Aerostatic Stability of a Long-Span Cable-Stayed Bridge Located in a Mountain-Gorge Terrain," *J. Aerosp. Eng.*, vol. 33, no. 3, 2020, doi: 10.1061/(ASCE)AS.1943-5525.0001117.

[11] A. Velazquez and A. Chowdhury, "Aeroelastic parameters of cable suspended bridges via computational fluid dynamics," presented at the AIP Conference Proceedings, 2023. doi: 10.1063/5.0177721.

[12] A. Heydari, "Investigating the flow around obstacles near the surface: clearance-controlled vortex shedding for four equal-diameter bridge-deck shapes," *J. Wind Eng. Ind. Aerodyn.*, 2025, [Online]. Available: https://www.sciencedirect.com/science/article/pii/S2590123025029512

[13] H. Tang, J. Kang, and Y. Li, "Aerostatic and aerodynamic stability of a suspension bridge during early erection stages," *J. Wind Eng. Ind. Aerodyn.*, vol. 233, 2023, doi: 10.1016/j.jweia.2022.105297.

[14] M. Rønne, A. Larsen, J. H. Walther, and S. V. Larsen, "Flutter stability of twin-box bridge decks," 2024. [Online]. Available: https://arxiv.org/abs/2410.17097

[15] S. Fan, W. Chen, H. Tang, and Y. Li, "Aerodynamic interference between two boxes in parallel arrangement and flow field characteristics around the girder," *Adv. Bridge Eng.*, vol. 3, no. 1, 2022, doi: 10.1186/s43251-022-00079-6.

[16] A. J. Álvarez and F. Nieto, "Vortex induced vibration analysis of a twin-box bridge deck by means of 3D LES simulations," *J. Wind Eng. Ind. Aerodyn.*, vol. 258, p. 106015, Mar. 2025, doi: 10.1016/j.jweia.2025.106015.

[17] J. Tan, "Life-cycle assessment for flutter probability of a long-span bridge," *Structures*, vol. 53, p. 106015, 2024, doi: 10.1016/j.istruc.2024.106015.

[18] L. Ming, Z. Longqi, Y. Congsen, and Y. Mei, "Flutter Performance Research of Π-Shaped Section Cable-Stayed Bridge," presented at the Advances in Transdisciplinary Engineering, 2023, pp. 609–614. doi: 10.3233/ATDE230340.

[19] H. Luo, W. Wu, Q. She, B. Li, C. Yang, and Y. Pan, "Thermal Effects on Main Girders During Construction of Composite Cable-Stayed Bridges Based on Monitoring Data," *Buildings*, vol. 15, no. 17, p. 2990, 2025, doi: 10.3390/buildings15172990.

[20] D. A. U. Absor, A. Aminullah, and B. Supriyadi, "Structural Health Assessment of Kretek II Bridge using Enhanced Frequency Domain Decomposition," *J. Civ. Eng. Forum*, vol. 10, no. 2, pp. 123–132, 2024, doi: 10.22146/jcef.9151.

[21] R. B. Panuntun, A. Aminullah, B. Suhendro, and P. K. Wardana, "Bridge Displacement Estimation using Tiltmeter Data," *J. Civ. Eng. Forum*, vol. 5, no. 2, 2019, doi: 10.22146/jcef.43670.

[22] S. Yadi, B. Suhendro, H. Priyosulistyo, and A. Aminullah, "Shake Table Test of Floating Cable-Stayed Bridge under Dynamic Excitation," *Int. J. Civ. Eng. Technol. IJCIET*, vol. 9, no. 11, pp. 2075–2090, 2019.

[23] R. Montoya, A. Kareem, and S. Hernandez, "Aero-structural design optimization of long-span bridges: From linear to nonlinear aeroelasticity-driven perspectives," presented at the Proceedings of the International Conference on Wind Engineering, 2023. doi: 10.48550/arXiv.2308.12345.